Effect of Operating Parameters on the Performance of Axially Rotating Horizontal Heat Pipe: Experimental Investigation

M.A. Yassin, H.M. Abd El-Hameed, M.H. Shedid, H. Abou-Ziyan

Mechanical Power Engineering Department, Faculty of Engineering, Mattaria
Helwan University, Cairo, 11718, Egypt.

Abstract

This experimental study investigates the thermal performance of axially rotating horizontal wickless heat pipes under different operating conditions. A heat pipe is designed, constructed, and tested for the investigation. The experiments are conducted on a heat pipe rotating at speeds of 250-1500rpm, with Taylor numbers ranging from 3.0×10^7 to 1.1×10^9, and heat fluxes from 2090 to 16700W/m^2. The heat pipe is charged with water as a working fluid, filling 100% of the evaporator volume. The effect of liquid charging is also examined, varying between 5 and 55% of the heat pipe's inner volume. The results demonstrate that rotation significantly enhances the heat pipe's performance. The effective thermal conductivity of heat pipes increases by 30-40% for heat flux ranging from 2090 to 8350 W/m^2, and approximately 20% for higher heat fluxes as the Taylor number increases from 3.0×10^7 to 1.1×10^9. The best performance of the rotating heat pipe is achieved at the highest Taylor number of 1.1×10^9 and the lowest heat flux of 2090 W/m^2, resulting in a remarkable 9.47-fold increase in effective thermal conductivity compared to copper. The study also identifies the optimum liquid charge for the heat pipe, which is found to be about 35% of the inner pipe volume.

Keywords: Rotating heat pipe, filling ratio, heat flux, heat transfer characteristics, heat pipe thermal performance.

1. Introduction

The heat pipe is a simple device that effectively removes heat by utilizing the processes of evaporation and condensation of a fluid with a saturation temperature suitable for the given application. Specifically, within the evaporator section, a charged fluid is evaporated at a notably high temperature, while in the condenser section, the resulting vapor condenses at a lower temperature. This process enables the heat pipe to efficiently transfer heat from its source to its destination [1,2]. The classical heat pipes have received considerable consideration to investigate their various aspects [3-7], including pipe size [8-10], pipe limitations [11-15], evaporator geometry enhancement [16-19], condenser geometry enhancement [20, 21], and others [22-26].

However, rotating heat pipes find important applications in cooling rotating equipment such as gas turbine blades and rotors, grinding machines, electric motors, etc. [27-29]. Rotating heat pipes are designed to leverage the centrifugal force they generate to facilitate the efficient removal of heat. This is achieved through the use of a charged working fluid that is circulated within the pipe. As the heat pipe rotates, the centrifugal force generated assists in moving the working fluid toward the outer regions of the heat pipe, where it can effectively exchange heat in the evaporator and condenser sections. This innovative approach to heat removal offers a highly effective solution for applications where traditional methods may be inadequate [28].

Rotating heat pipes are classified into two primary types: radial and axial as shown in Fig. 1. Radial rotating heat pipes feature an evaporator and condenser that are separated in a radial direction, causing the centrifugal force to be parallel to the fluid flow [30]. This allows compensated liquid to move from the condenser section to the evaporator section, facilitating efficient heat removal. In contrast, the axial rotating heat pipe features an evaporator and condenser that are separated parallel to the rotation axis [30]. This results in the direction of the centrifugal force normal to the axis of rotation. This unique configuration offers distinct advantages in specific applications, making it a valuable tool in heat removal technology [31].

Radial rotating heat pipe **Axial rotating heat pipe**
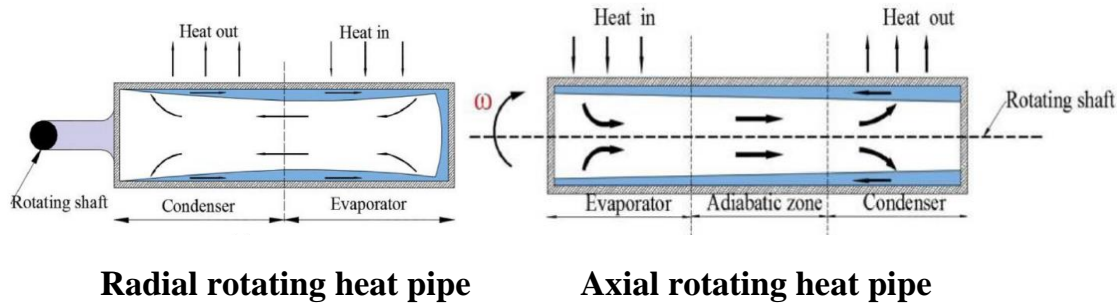
Fig. 1: Schematic of radial and axial rotating heat pipes.

It is worth noting that the effectiveness of a heat pipe is often quantified in terms of its effective thermal conductivity, thermal resistance, and effective heat transfer coefficient [32]. Among those is the 'equivalent thermal conductivity,' which measures how well the heat pipe can transfer heat relative to a solid material rod with similar dimensions [33]. This metric is a critical factor in evaluating the performance of a heat pipe and is commonly used in the design and optimization of heat transfer systems [32].

Xie et al. [34] experimentally compared the effect of rotation speed on the axial rotating heat pipe with a classical pipe without heat pipe at the same rotational speed. The authors reported high condenser temperature differences between cases of the heat pipe and the classical pipe, and higher thermal performance occurred due to the heat pipe's existence.

Lian et al. [35] numerically studied the effect of rotating speed from 2000 to 4000 rpm on the performance of heat pipes at applied heat ranging from 200 to 700 W. The results indicated that the overall thermal resistance slightly reduced as the applied heat rate increased. The thermal performance of the heat pipe improved obviously as the rotational speed increased using natural convection on the condenser section. On the other hand, Chang et al. [36] studied numerically the effect of fluid charges of 15 and 10.5 g, as well as rotational speeds ranging from 1000 to 5000 rpm, on the performance of axial rotating heat pipes at heat rates ranging from 100 to 900 W. Chang et al. results [36] concluded that increasing the rotational speed significantly enhanced the performance of axial rotating heat pipes. Also, their results showed a minor change in temperature along the rotating heat pipe, for the two tested fillings of fluid.

Low heat rates up to 25 W were experimentally studied by Denkena et al. [37] at rotational speeds from 2000 to 8000 rpm. Denkena et al. concluded that higher rotational speeds result in higher centrifugal forces, which yield better effective thermal conductivity of heat pipes. Additionally, their results showed that

a significant increase in thermal conductivity was noticeable between 3,000 rpm and 5,000 rpm for a heat input of 25 W, and between 5,000 rpm and 6,500 rpm for a heat input of 15 W.

In 2018, Panchal [38] developed an experimental work to study the effect of the filling ratio on the heat pipe performance. The results of those experiments showed that increasing the charge by more than 70% of the evaporator volume has recorded better performance for heat pipe in terms of increased heat transfer coefficient, decreased thermal resistance, and reduced temperature difference across the evaporator and condenser. Also, the results reported better performance achieved for filling ratios from 83 to 100% of the evaporator volume.

In order to investigate the impact of rotation speed (2000, 3000, and 4000 rpm) on the heat transfer characteristics of axial RHP, Song et al. [1] carried out an experiment. The temperature differential between the evaporator and condenser is used to study the heat transfer of the tapered HP for the three different fluid charges (9.2, 18.2, and 32 g). It is found that the fluid loading affects the rate at which heat is transferred as the rotating speed increases. When the rotating speed increases for the lower fluid charge, the heat transfer rate for a certain temperature drop increases. This is predicted because the condenser's liquid layer would thin as a result of the increased rotating speed caused by the component of centrifugal force parallel to the liquid flow direction. However, the increase in heat transfer with rotational speed is not as significant for the larger fluid loadings. This is primarily because at higher fluid loadings the excess fluid pools in the condenser.

Among the applications of rotating heat pipes, electric motors are the focus of the present work. Electric motors are essential components in many industrial applications, where their performance is significantly affected by the increase in their temperatures. Excessive heat causes mechanical and electrical motor components to deteriorate and the electric motor efficiency to reduce. Traditional water and oil cooling methods have been used for decades but have many limitations, particularly, these methods can be complex, expensive, and prone to sealing issues [39]. By utilizing rotating heat pipes for motor cooling, a more efficient and cost-effective solution that can improve motor performance and extend its lifespan is achieved [28, 40].

Previous literature reviews have indicated that despite the relatively considerable work in radial rotating heat pipes conducted before, there is a relative lack of research on the performance characteristics of axial rotating heat pipes. This conclusion was further confirmed by Li and Liu [30] in their review paper.

Interestingly, there appears to be a notable absence of studies focusing on low and moderate rotational speeds at low heat transfer rates. This range of low speed and heat flux in axially rotating heat pipes exists in many engineering and industrial applications such as electric motors, horizontal grinding machines, etc.

Therefore, the main objective of this study is to investigate the performance of axially rotating wickless heat pipes in the low ranges of rotational speeds and heat flux. An experimental heat pipe was designed, constructed, and tested considering the heat pipe limitations of operation. Effects of rotation speed (from 250 to 1500 rpm) and heat flux (from 2090 to 16700 W/m^2) are considered using water for a filling ratio of 100% of the evaporator volume. Also, the effect of volume charge on the performance of the heat pipe is investigated for filling ratios from 5 to 55% of the internal heat pipe volume. This investigation will provide valuable insights into the performance characteristics of axially rotating heat pipes, with potential applications in a wide range of industries. also, the results of this study facilitate the design of effective cooling systems for applications that use axially rotating heat pipes in low rotating speed and heat flux ranges.

2. Experimental Apparatus and Data Analysis

2.1 Heat Pipe Limitations

The current study investigates the performance characteristics of axially rotating heat pipes. To achieve this objective new heat pipe was designed, manufactured, assembled, and equipped with the necessary instruments. The dimensions of the heat pipe were selected considering the heat transfer limitations that are associated with the working fluid filling ratio. Similar to capillary heat pipes, fluid dynamic considerations dominate in determining the rotating heat pipes heat transfer limits [32]. These limitations include fluid entrainment, boiling process, and sonic and viscous limits, and the combination of the limits defines the heat pipe operating range [12-15]. The operating limits of the considered heat pipe filled with water, which occupies 100% of the evaporator volume (equivalent to 25% of the internal pipe volume), are 3.69, 10.7, and 4.07kW for the sonic, boiling, and fluid entrainment limits, respectively.

2.2 Description of the Experimental Apparatus

A schematic diagram of the experimental apparatus used in this work is illustrated in Fig. 2, showing the main components of the experimental apparatus. The heat pipe employed in the experiment is a wickless brass tube measuring 600 mm in length, 25.4 mm outer diameter, and 3 mm in thickness. The heat pipe is

divided into three main sections: the condenser, adiabatic, and evaporator. The evaporator and condenser sections are of equal length, measuring 150 mm each, while the adiabatic section is 300 mm in length. The characteristics of the heat pipe are tabulated in Table 1.

As can be seen in Fig. 2, the evaporator end of the heat pipe is connected to a stainless-steel external rod through a coupling. The external rod is equipped with a power slip ring and a measurement slip ring. The power slip ring is utilized to provide electric power to the electric heater during rotation. Also, the heat pipe is supported between two ball bearings (GG.ASE07-E INA) to facilitate its rotation. A variable-speed electric motor with a power rating of 0.75 kW was used to rotate the heat pipe using a pully-belt assembly. The speed of the electric motor is controlled using a digital inverter to provide rotational speeds ranging from 250 to 1500 rpm, with a step of 250 rpm. A laser-cut rigid iron base of 6mm thick supports the heat pipe setup and helps to isolate the vibration due to the heat pipe rotation.
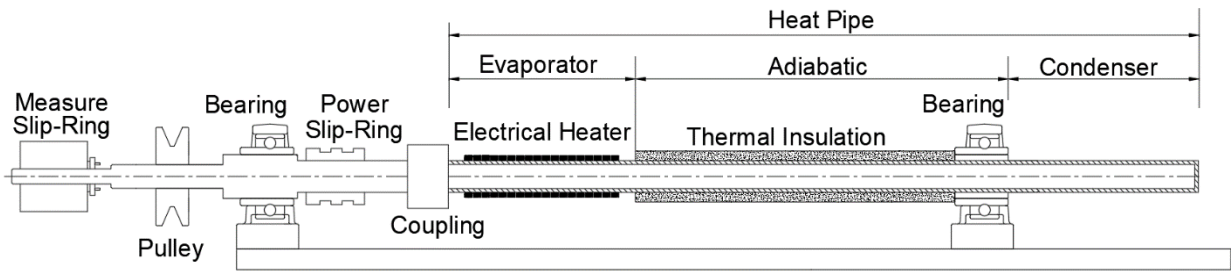
Fig. 2: Schematic diagram of the experimental apparatus.

Table 1. Heat pipe characteristics

Pipe characteristics	Value
Pipe Material	Brass
Evaporator length, mm	150
Adiabatic section length, mm	300
Condenser length, mm	150
Outer diameter, mm	25.4
Inner diameter, mm	19.4
Working fluid	Water
% Charge of evaporator volume	100

The evaporator section is equipped with an electric heater with a power rating of 1 kW. The input power is provided to the electric heater using a voltage regulator device (2 KVA). The electric heater is winded around the evaporator, and

a high thermal conductive material is used to ensure perfect contact between the heater and the evaporator surface. The high-conductive material, in the form of powder, fills gaps between the evaporator surface and the heater coil. The evaporator and adiabatic sections are insulated with a 25 mm thick layer of ceramic fiber insulation. Applying a heat rate on the evaporator section generates vapor inside the pipe that moves from the evaporator to the condenser through the adiabatic section. The condenser is cooled by an axial fan (500004487 - Fresh) with a flowrate of 3260 CFM. The fan helps to enhance heat dissipation from the condenser by increasing the airflow over its surface. In the condenser section, the vapor condenses by dissipating heat to ambient air at a constant temperature. Thus, the condenser receives heat from the heat pipe evaporator, allowing the transfer of heat from the heat source to the environment. The experimental apparatus is carefully designed to ensure accurate and reliable experimental runs enabling the investigation of the performance characteristics of axially rotating heat pipes under different operating conditions.

The experimental apparatus is equipped with the necessary instrumentation and data logger. Six pre-calibrated type-T thermocouples have been installed along the entire length of the heat pipe, with two thermocouples for each section, to measure the outer surface temperature of each section of the heat pipe. The measurement slip ring receives signals from thermocouples that are fixed at the heat pipe surface and transfers them to the data loggers. Another thermocouple of the same type was used to monitor the ambient temperature. To monitor the surface temperature, throughout the experimental run, the measurement slip ring is used to connect thermocouples to digital thermometer readers capable of reading 0.1°C, with an error percentage of slip ring reading averaging ±0.1 K.

2.3 Experimental Procedures

The heat pipe sections are manufactured from a 25.4mm diameter brass rod, and the extension rod from a 25.4mm diameter stainless steel rod. A dedicated CNC machine is used to ensure accurate dimensions and reliable straightening of the heat pipe. The heat pipe setup necessitates alignment of the heat pipe with its accessories several times using a professional laser kit to avoid misalignment, excessive heat, and vibration of the heat pipe that may cause errors in predicting the performance of the heat pipe. The apparatus commissioning is conducted carefully to guarantee reliable and accurate experimental runs to assess the performance of the axially rotating heat pipe.

Before starting the experiment, the heat pipe is connected to a vacuum pump (DV-4E Eliminator 4 cfm), which typically requires more than 30 to 45 minutes to evacuate the pipe from moisture and non-condensable gases that influence the evaporation and condensation processes in the heat pipe. Then, the required amount of water is charged in the heat pipe using an accurate balance. To minimize the presence of non-condensable gases (NCG), the water is pre-heated before being introduced into the heat pipe. This pre-heating process helps to ensure the purity of the water and reduces the likelihood of NCG formation within the system [41, 42].

The experiment is started by fixing the heat pipe speed at a prescribed value using the variable speed motor and the pully assembly. After setting the heat pipe speed, the input power on the evaporator section is applied using the voltage regulator and the electric heater. The heat pipe is allowed to run until steady-state conditions are achieved. The steady state is monitored through thermocouple readings and requires 3 to 5 hrs for each run. After acquiring the data for the experiment, the heat input to the evaporator is changed to the next value until the experiments are performed for all input heat that ranges from 25-200W (equivalent to 2090 - 16700 W/m^2), using a step of 25 W. Then, the heat pipe speed is changed for the next reading, and the experiments are performed for all heat inputs. The heat pipe speed varies from 250 to 1500 rpm, with a step of 250 rpm. However, the effect of filling ratios was investigated from 5 to 55%, with a 10% increment, at two rotation speeds of the heat pipe using two heat inputs for each speed.

The experimental program involves the effects of rotation speed, heat flux, and filling ratio on the thermal performance of an axially rotating heat pipe. The ranges and conditions of the experimental program are listed in Table 2. Eight heat fluxes are experimented with each of the six rotation speeds (48 runs). On the other hand, seven filling ratios have experimented with two rotation speeds for two heat flux values (28 runs).

Table 2. Experimental work operating parameters

Parameters	Considered values
Rotational Speed (N, rpm)	250, 500, 750, 1000, 1250, and 1500
Heat input, Q (W) corresponds to heat flux (q, W/m^2)	25 (2090), 50 (4175), 75 (6260), 100 (8350), 125 (10440), 150 (12530), 175 (14615), and 200 (16700)
Filling ratio (relative to the inner volume of the pipe)	5, 15, 25, 35, 40, 45, and 55%

2.4 Experimental Data Analysis

For each experimental run, the average wall temperatures for the evaporator, condenser, and adiabatic sections of the heat pipe are evaluated as the average of the two measured temperatures of the outer surface of the heat pipe using thermocouple readings by equations 1, 2, and 3, respectively.

$$T_e = \frac{T_1 + T_2}{2} \tag{1}$$

$$T_a = \frac{T_3 + T_4}{2} \tag{2}$$

$$T_c = \frac{T_5 + T_6}{2} \tag{3}$$

As the heat flows from the evaporator to the condenser, it produces a temperature difference between both sections. The average ΔT between the evaporator and condenser sections determines the performance of the heat pipe and is determined using equation 4.

$$\Delta T = T_e - T_c \tag{4}$$

Taylor number (Ta) is a crucial dimensionless quantity that highlights the significance of centrifugal forces, or inertial forces resulting from fluid rotation around an axis, relative to viscous forces [43, 44].

$$Ta = \frac{4\omega^2 R^4}{\nu^2} \tag{5}$$

Where ω is the angular velocity of the fluid defined as ω=2πn/60 with n the rotational speed of the heat pipe, R is the inner radius of the heat pipe, and ν is the kinematic viscosity of the fluid.

The thermal resistance of the heat pipe is one of the parameters describing the thermal performance of the heat pipe. The heat pipe's thermal resistance (R_{th}) can be calculated by the following equation [45, 46].

$$R_{th} = \frac{T_e - T_c}{Q} \tag{6}$$

In addition to thermal resistance, effective thermal conductivity (k_{eff}) is a critical parameter that characterizes the thermal performance of heat pipes. As a defining

property of heat pipes, k_{eff} is determined by combining various effects and can be calculated using Equation 7 [37].

$$k_{eff} = \frac{Q \cdot L_{eff}}{A_c \cdot (T_e - T_c)} \tag{7}$$

Where:

Q Applied rate of heat flow (W)

L_{eff} The heat pipe effective length (m).

$$L_{eff} = \left(\frac{L_e + L_c}{2}\right) + L_a$$

A_c Heat pipe cross-sectional area (m^2).

$$A_c = \frac{\pi}{4}D^2$$

T_e The average surface temperature of the evaporator (K).

T_c The average surface temperature of the condenser (K).

Hence, the applied heat is the difference between the input heat (Q_{in}) and the heat losses (Q_{loss}) from the evaporator and adiabatic sections. The heat loss from the evaporator and adiabatic sections ranges from 3.8 to 6.25% of the total heat input. For each section, the heat loss is calculated using the following equations.

$$Q_{loss} = Q_{loss,ev} + Q_{loss,cond} \tag{8}$$

$$Q_{loss} = \frac{(T_{ev} - T_{amb})}{R_{ev}} + \frac{(T_{ad} - T_{amb})}{R_{ad}} \tag{9}$$

$$R = \left(\frac{1}{hA_o}\right) + \frac{\ln(r_o/r_i)}{2\pi l k_i} \tag{10}$$

Where T_{ev} or T_{ad} is the surface temperature of the evaporator or condenser sections, T_{amb} is ambient temperature, and R_{ev} or R_{ad} is the thermal resistance of the evaporator or adiabatic section. Also, h is the convection heat transfer coefficient from the insulation surface to air, A_o is the outer surface area of the insulation, r_o and r_i are the outer and inner radius of the insulation, l is the length of the evaporator or adiabatic section, and k_i is the thermal conductivity of the insulation.

2.5 Uncertainty Analysis

The uncertainty analysis is conducted according to the method defined by Kline and McClintock [47] and modified by Moffat [48]. Table 3 presents the maximum uncertainty in the specified parameters.

For one variable: Consider a variable X_i, which has a known uncertainty δX_i.

The form for representing this variable and its uncertainty is $X_i = X_i$ (measured) $\pm$ δX_i

The basic equation of uncertainty analysis is equation 11. Each term denotes the amount that the uncertainty in a single variable, δX_i, contributed to the overall uncertainty of the result, δR.

$$\delta R = \left(\sum_{i=n}^{n} \left(\frac{\partial R}{\partial X_i} \delta X_i \right)^2 \right)^{1/2} \tag{11}$$

Table 3: Maximum uncertainties of measured parameters and derived quantities

Parameter	%Uncertainty
Measured temperature	1.29
Temperature difference	2.58
Input power	0.28
Rotation speed	0.09
Heat flux	4.01
Effective thermal conductivity	4.77
Thermal resistance	2.60
Taylor number	3.94

3. Results and discussion

The results of the experimental tests conducted in this study aimed to investigate the performance of axially rotating heat pipes. The results cover a range of heat flux from 2090 to 16700 W/m^2, and rotation speed from 250 to 1500 rpm, which corresponds to Taylor numbers from 3.0×10^7 to 1.1×10^9. The experiments were conducted using water as a working fluid at a fixed charging ratio of 25% of the inner pipe volume, which is equivalent to 100% of the evaporator volume. Also, the effect of the water charging ratio is investigated from 5% to 55% of the inner pipe volume. Those effects will be presented in the following subsections.

3.1 Effect of rotation speed

Figures 3a and 3b present a sample of the temperature distribution on the outer surface of the heat pipe at the lowest (2090 W/m^2) and highest tested (10440 W/m^2) heat fluxes, respectively, for various rotation speeds ranging from 250 to 1500 rpm. Along the heat pipe, the evaporator temperature is higher than the adiabatic section, which is, in turn, higher than the condenser section. The difference between the evaporator and condenser temperatures depends on the

applied heat flux and the rotational speed. For both heat fluxes in Figs. 3a and 3b, the surface temperatures along the heat pipe decrease with increasing the rotation speed. This trend is particularly evident when comparing the curves for lower rotation speeds (e.g., 250 rpm) with those for higher rotation speeds (e.g., 1500 rpm).

Figure 3 illustrates that at either heat flux of 2090 or 10440 W/m^2, as the rotational speed increases the surface temperature decreases, particularly at higher heat flux. The decrease in the heat pipe surface temperature with increasing rotational speed can be attributed to the increased centrifugal force and turbulence generation. The increase in centrifugal force pushes more liquid to the evaporator surface, which enhances the rate of evaporation for the same heat flux. Also, the increase in rotational speed improves the heat transfer from the condenser surface to the surrounding fluid because of the enhanced heat transfer coefficient as the speed increases.
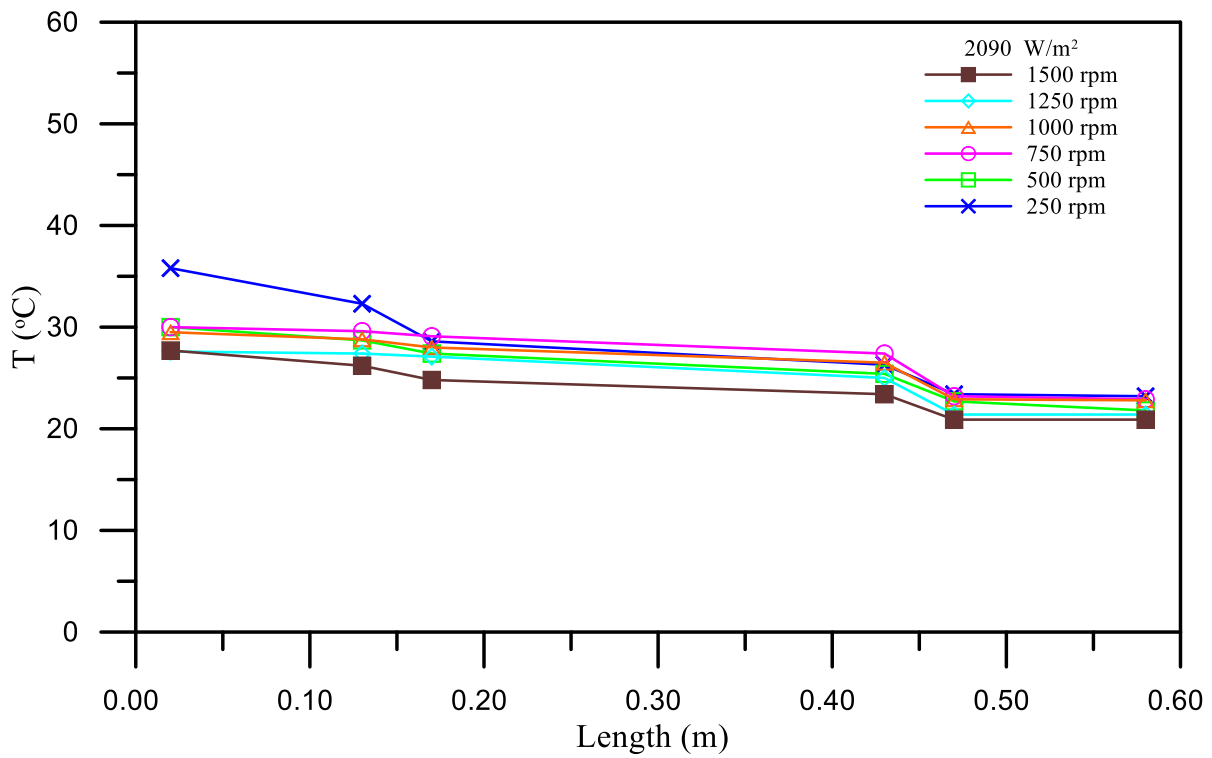

(a)
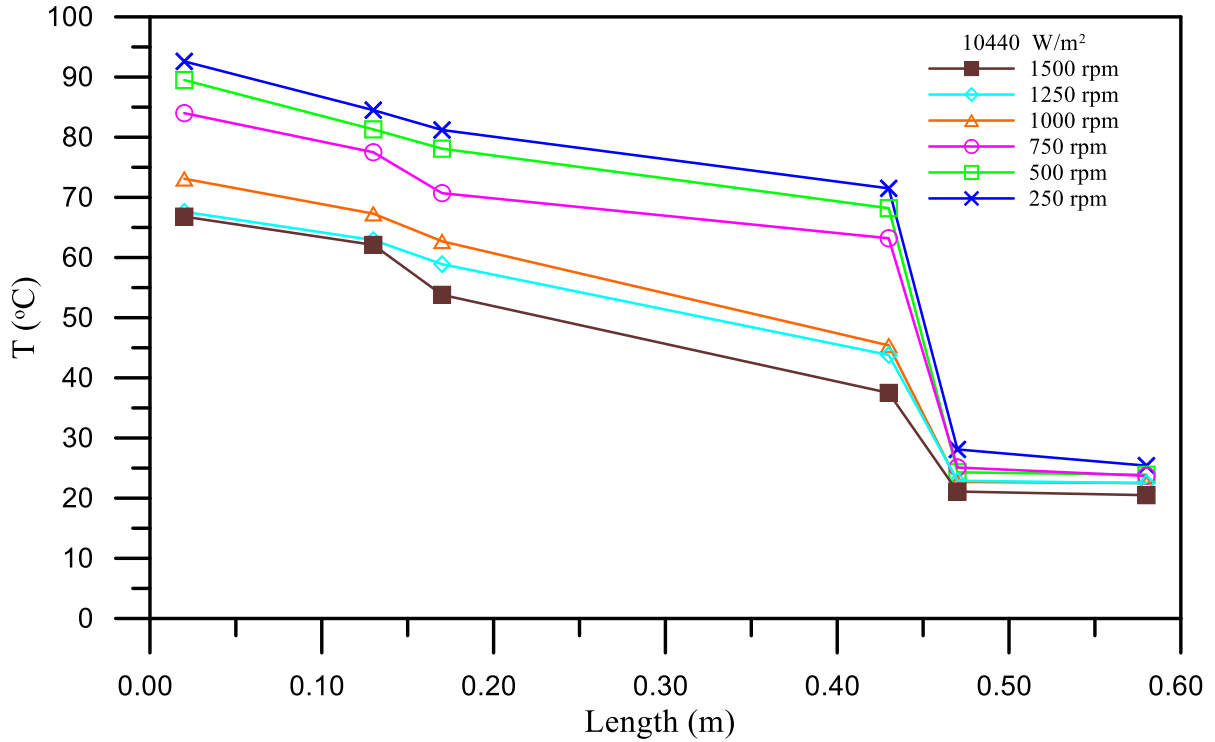
(b)

Fig. 3: Temperature distribution along heat pipe for different rotational speed at heat fluxes of (a) 2090 and (b) 10440 W/m^2.

The heat pipe performance significantly depends on the temperature difference between the evaporator and condenser sections. Figure. 4 depicts this temperature difference (ΔT), as a function of the rotational speed (N), for the tested heat fluxes. Generally, the temperature difference decreases by 23-43% for the highest and lowest tested heat flux as the rotational speed increases from 250 to 1500 rpm. Thus, the results demonstrate the significant impact of rotational speed on reducing the temperature difference between the evaporator and condenser in heat pipes, leading to more efficient heat transfer and uniform temperature distribution along the heat pipes.
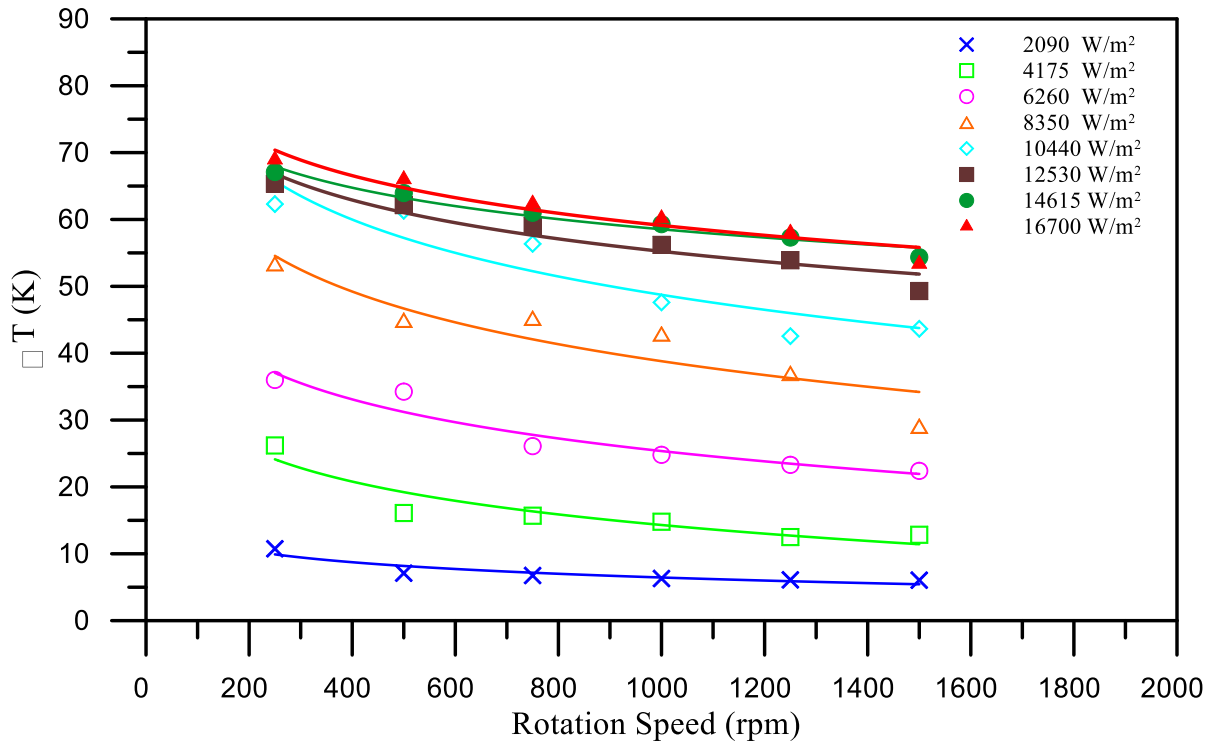
Fig. 4: Temperature difference between evaporator and condenser at different heat flux and rotational speeds.

3.2 Effect of Heat Flux

Comparing Figs. 3a and 3b provide insights into the effect of heat flux on the surface temperature distribution. Figure. 3a shows that the surface temperature decreases by approximately 15 to 27% as the rotational speed increases from 250 to 1500 rpm for a heat flux of 2090 W/m^2. Similarly, Fig. 3b shows that the surface temperature decreases by approximately 16 to 47% as the rotational speed increases from 250 to 1500 rpm for a heat flux of 10440 W/m^2. These results demonstrate that the effect of rotational speed on the surface temperature distribution becomes more pronounced with increasing heat flux. This trend can be attributed to the increased rate of evaporation and condensation (formation of bubbles and droplets) at the higher heat flux due to the significant effect of the centrifugal force.

Figure 4 shows the temperature difference increases with heat flux for a given rotational speed. The decrease in temperature difference when the rotational speed increases from 250 to 1500 rpm is about 43% for the lowest heat flux of 2090 W/m^2, 30% for a higher heat flux of 10440 W/m^2, and 23% for the highest heat flux of 16700 W/m^2. However, the level of temperature difference increases as the heat flux increases. In other words, the reduction in temperature difference is about 5, 20, and 15°C for the stated heat fluxes, respectively. Thus, the reduction in

temperature difference increases as the heat flux increases up to a value of 10440 W/m^2, then decreases at higher heat flux. This trend is indicated by the slope of the curves in Fig. 4, as the curves for the higher two heat flux coincide at high rotational speeds. In conclusion, the effects of heat flux and rotational speed on the temperature difference are significant.

3.3 Effect of Taylor Number

The effect of Taylor number on the temperature difference between the evaporator and condenser at different heat fluxes is illustrated in Fig. 5. As the Taylor number increases, the temperature difference between the evaporator and condenser decreases. For example, at a heat flux of 16700 W/m^2, the temperature difference decreases by 4.3, 9.6, 12.8, 15.9, and 22.6% when the Taylor number increases from 3.0×10^7 to 1.2×10^8, 2.7×10^8, 4.9×10^8, 7.6×10^8, and 1.1×10^9, respectively.

Heat pipe rotation has a profound impact on reducing the temperature difference between the evaporator and condenser in a heat pipe. This effect can be attributed to the mechanism of the two-phase flow inside the heat pipe, which is significantly influenced by the centrifugal force generated by the rotation. At low rotational speeds, the flow is mainly driven by surface tension and gravity, leading to a slug-plug flow pattern. As the rotational speed increases, the centrifugal force becomes dominant, causing the two-phase flow to become an annular flow pattern [30]. This transition results in a substantial increase in the interfacial area and turbulence, which significantly enhances the heat transfer rate between the working fluid and the heat pipe wall.

The separation of the liquid and vapor phases due to the centrifugal force generated by the rotation of the heat pipe leads to a thinner liquid film and a larger interfacial area. This separation significantly enhances the evaporation and condensation heat transfer rates, ultimately resulting in a remarkable reduction in the temperature difference between the evaporator and condenser. Moreover, the increase in the interfacial area due to rotation also boosts the capillary pressure, which counteracts the pressure drop and maintains a near-constant liquid-vapor interface temperature in the evaporator and condenser sections [30].
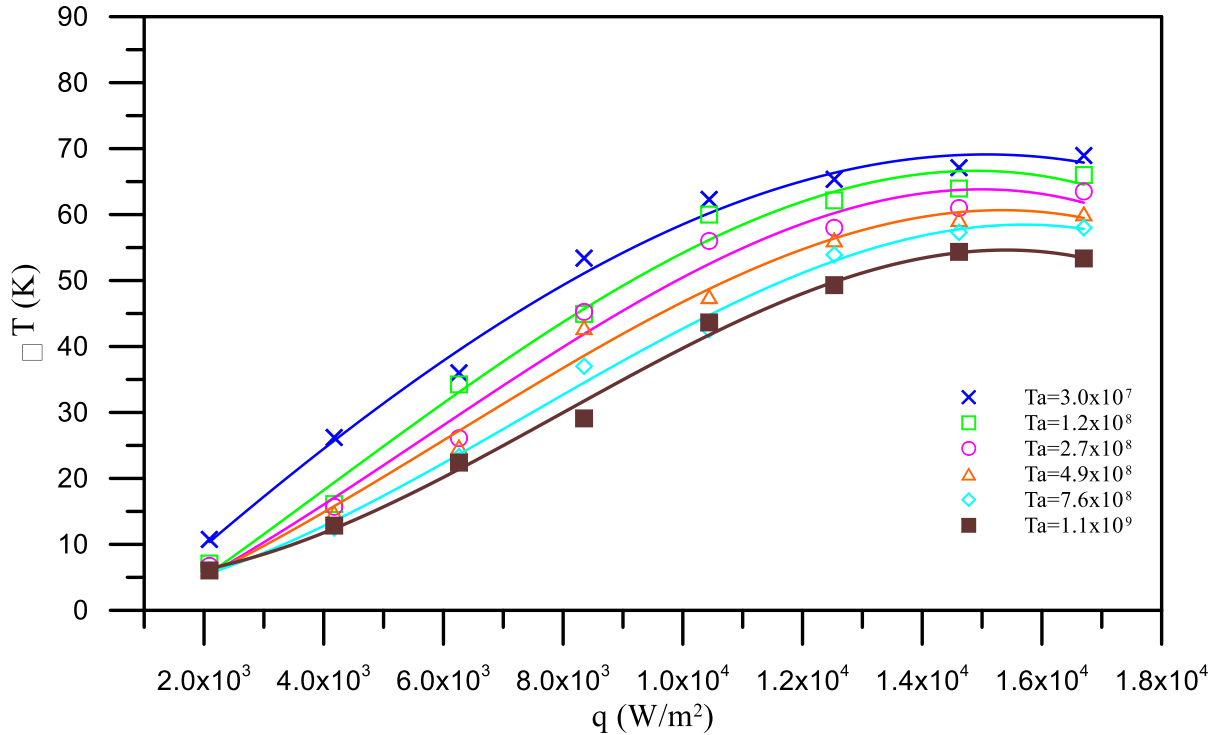
Fig. 5: Temperature difference between evaporator and condenser at different heat flux and Taylor number.

3.4 Effect of speed and heat flux on heat pipe performance

Effective thermal conductivity and thermal resistance, as defined in equations 6-7, respectively, are widely used to express the performance of rotating heat pipes, as they offer a clear and concise way to assess the efficiency of the devices.
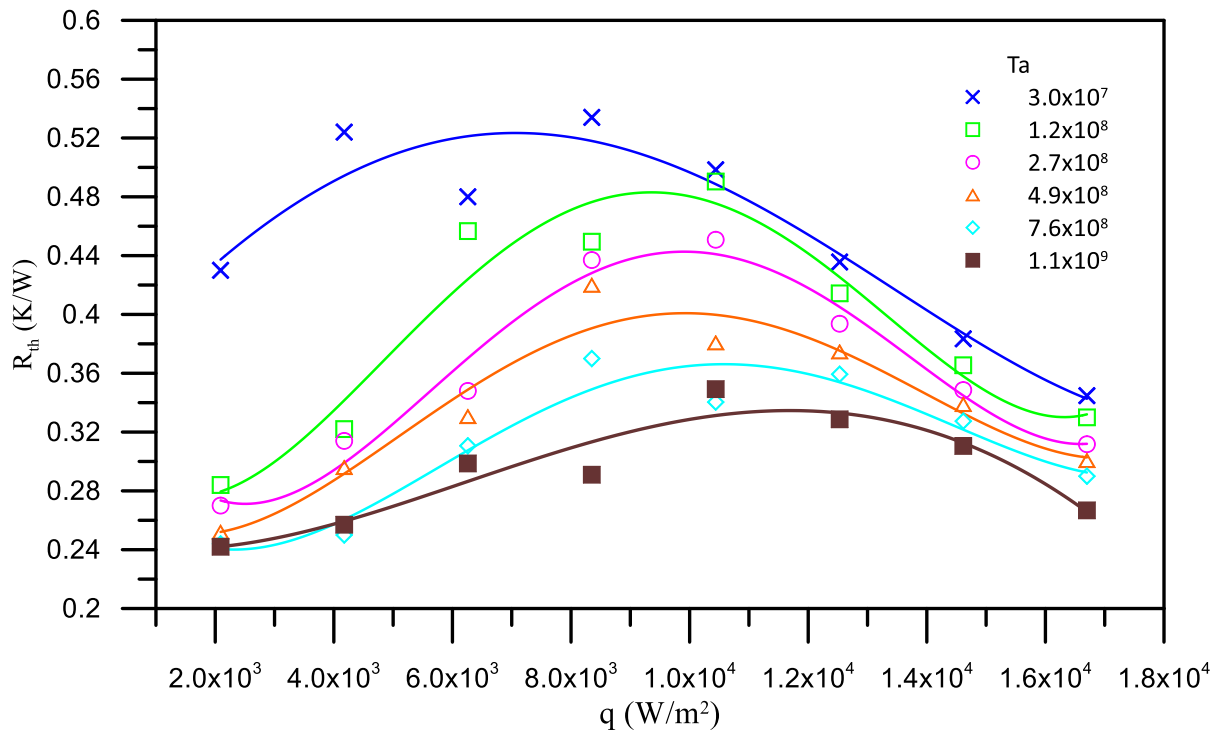
3.4.1 Thermal Resistance

Figure 6 shows the thermal resistance of the heat pipe at different Taylor numbers and rates of heat flux. For any Taylor number, the thermal resistance increases with heat flux up to a moderate value and then decreases at higher heat fluxes. The reason behind this trend is that for low heat inputs, the decrease in the temperature difference is lower than the increase in heat inputs resulting in a remarkable reduction in the thermal resistance. Additionally, another factor contributing to the increase in thermal resistance at low heat fluxes is the possibility of having a portion of the fluid that has not undergone boiling and condensation, treating it as a single-phase flow. However, at high heat flux, this possibility diminishes, leading to the disappearance of this phenomenon. On the other hand, the rate of increase in the temperature difference at higher heat flux is lower than

the rate of increase in the heat inputs. Thus, the thermal resistance decreases as the heat rate increases.

The thermal resistance significantly decreases as the Taylor number increases for each applied heat flux. For instance, at a Taylor number of 1.1×10^9, the thermal resistance decreases than at a Taylor number of 3.0×10^7 by an outstanding ratio of 44, 51, 38, and 46% (average of 44.75%) at low heat fluxes of 2090, 4175, 6260, and 8350, respectively. Furthermore, at high heat fluxes of 10440, 12530, 14615, and 16700, the thermal resistance decreases by 30, 25, 19, and 23% (average of 24.25%), respectively, as a Taylor number decreases from 1.1×10^9 to 3.0×10^7. Therefore, the thermal resistance of the heat pipe demonstrates a more significant decrease rate for lower heat inputs than for higher ones. This trend is depicted by the large gap between curves of different Taylor numbers at low heat flux compared to high heat flux (see Fig. 6).

The decrease in the thermal resistance with increasing heat flux is in agreement with Lian et al. [35] as they reported that the overall thermal resistance slightly reduced as the applied heat rate increased.
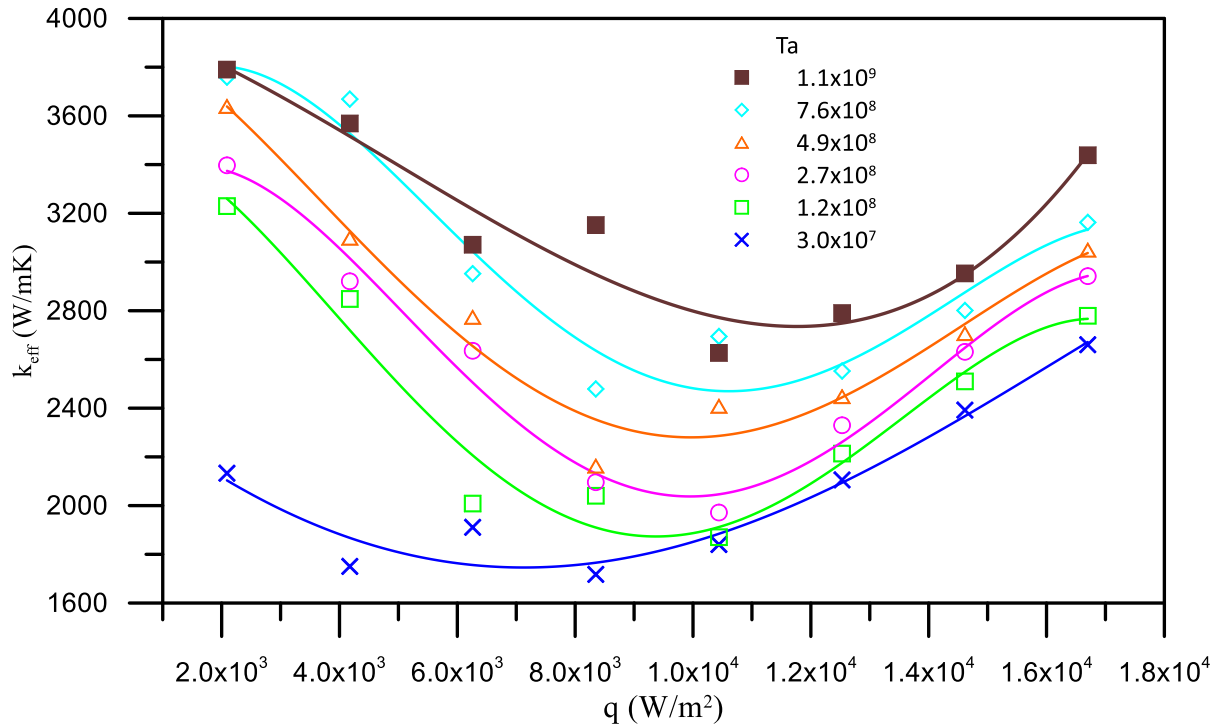

Fig. 6: Thermal resistance of heat pipe at different Taylor numbers and heat fluxes.

3.4.2 Thermal Conductivity

The effective thermal conductivity for different Taylor numbers and heat fluxes is presented in Fig. 7. The effective thermal conductivity of the heat pipe is inversely proportional to the thermal resistance ($k_{eff} = L_{eff}/A_c \times R_{th}$). Therefore, the trends of the effective thermal conductivity shown in Fig. 7 are opposite to those in Fig. 6. It decreases for all Taylor numbers up to a specific heat flux and then, increases until the highest tested heat flux. The increase in Taylor number enhances the effective thermal conductivity of the heat pipe, particularly at low heat fluxes. As Taylor numbers are increased from 3.0×10^7 to 1.1×10^9, the effective thermal conductivity increases by 30 to 40% for heat flux from 2090 to 8350 W/m^2, and about 20%, in average, for the higher heat fluxes, as shown in Fig. 6. The explanation for the trends of the percentage difference increase in the effective thermal conductivity is similar to that discussed for the thermal resistance, i.e., depends on the rate of change in both heat rate (Q), and the evaporator to condenser temperature difference (ΔT).

The enhancement of the heat pipe performance due to the increase of Taylor number (or the heat pipe rotational speed) agrees with the results reported by Lian et al. [35], Chang et al. [36], and Denkena et al. [37].

In conclusion, the best performance of heat pipes corresponds to the lowest thermal resistance or the highest effective thermal conductivity. Therefore, higher Taylor numbers produce lower resistances and higher thermal conductivities than lower Taylor numbers. Also, low heat fluxes provide better performance than medium heat fluxes. The lowest heat pipe performance takes place at heat fluxes ranging from about 7000 to 10000 W/m^2, depending on the Taylor number. It is to be noted that the performance of the tested heat pipe is better than a copper rod by 4.3 to 9.47 folds.

Fig. 7: Effective thermal conductivity of heat pipe at different Taylor numbers and heat fluxes.

3.5 Effect of Charging Ratio

The effect of the working fluid charge on the thermal performance of heat pipes is investigated for filling ratio from 5% to 55% of the inner pipe volume, at two rotational speeds (250, 1500 rpm), which is equivalent to Taylor numbers of 2.7×10^8 and 1.1×10^9, for two values of heat flux of 10440 W/m^2 (Figs. 8a and 9a) and 16700 W/m^2 (Figs. 8b and 9b).

Figures 8a and 8b depict a sample of the temperature distribution on the outer surface of the rotating heat pipe at different filling ratios and two heat fluxes of 10440 W/m^2 and 16700 W/m^2, respectively. For low heat flux with both Taylor numbers (Fig. 8a), the highest evaporator and adiabatic temperature occur for a filling ratio of 5% and the highest condenser temperature for a filling ratio of 35%. On the other hand, the lowest evaporator and adiabatic temperatures take place at a filling ratio of 35% and condenser temperature at a filling ratio of 55%. For high heat flux (Fig. 8b) the highest and lowest evaporator and adiabatic temperature are at filling ratios of 5% and 35%, respectively. Also, the highest and lowest condenser temperatures are for filling ratios of 35% and 55%, respectively.

The results in Fig. 8 indicate that the temperature distribution becomes more uniform at a filling ratio of 35%. As the filling ratio deviates from this value, the

temperatures within the evaporator and adiabatic sections of the heat pipe increase, and the temperature distribution becomes increasingly non-uniform on the surface of the heat pipe. This finding highlights the importance of selecting an appropriate filling ratio to avoid excessive temperature gradients and ensure efficient heat transfer.
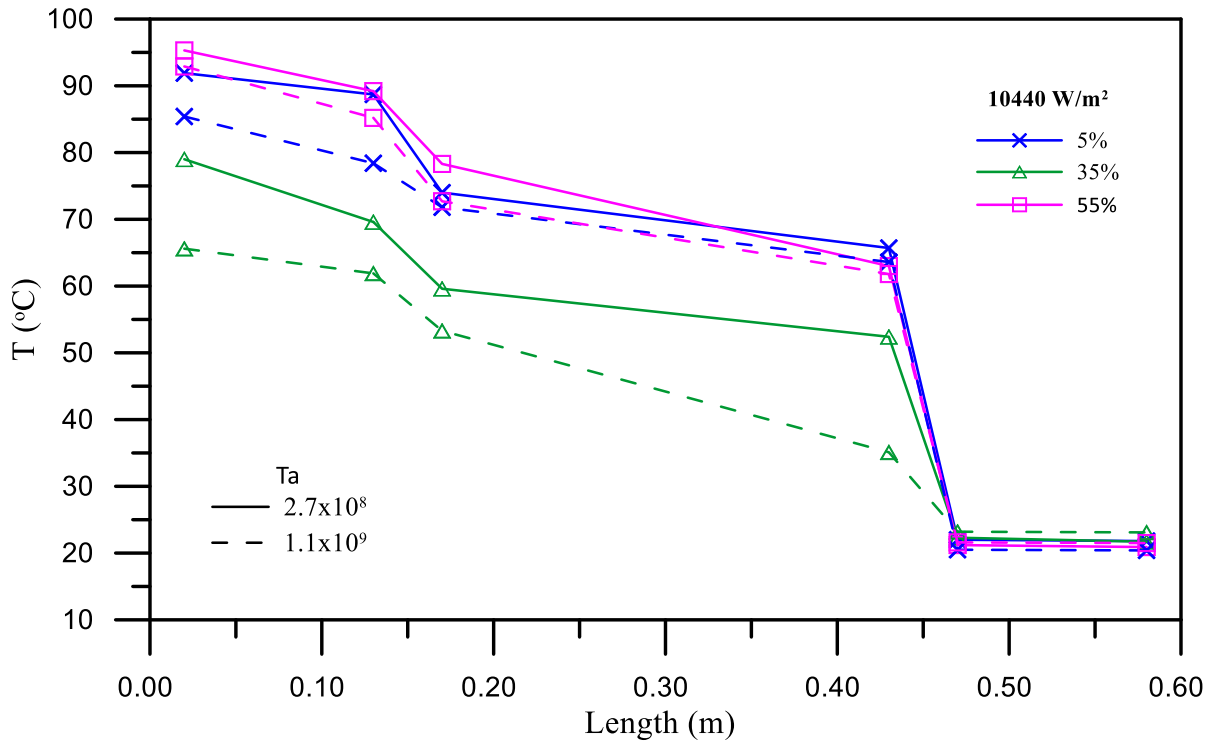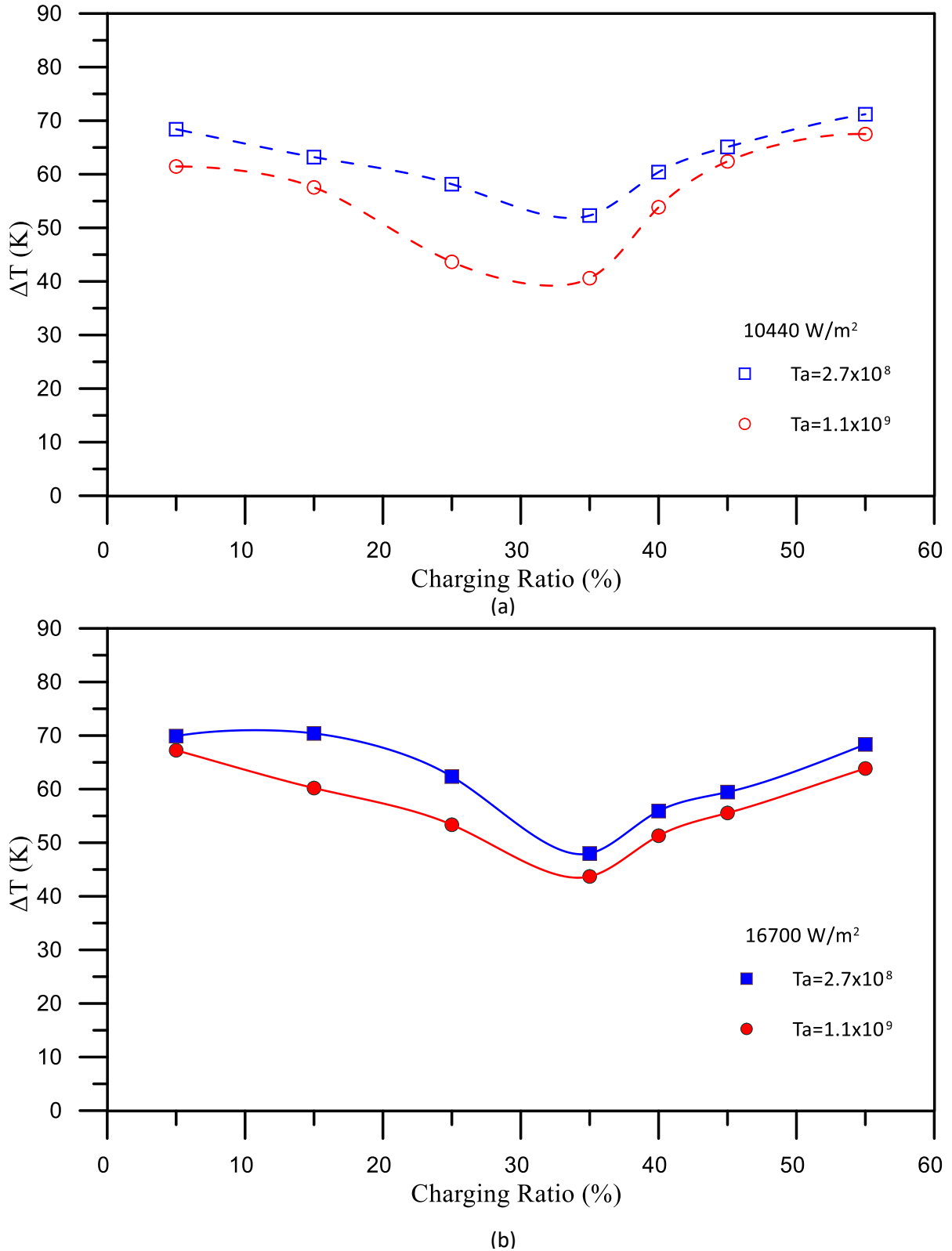

(a)
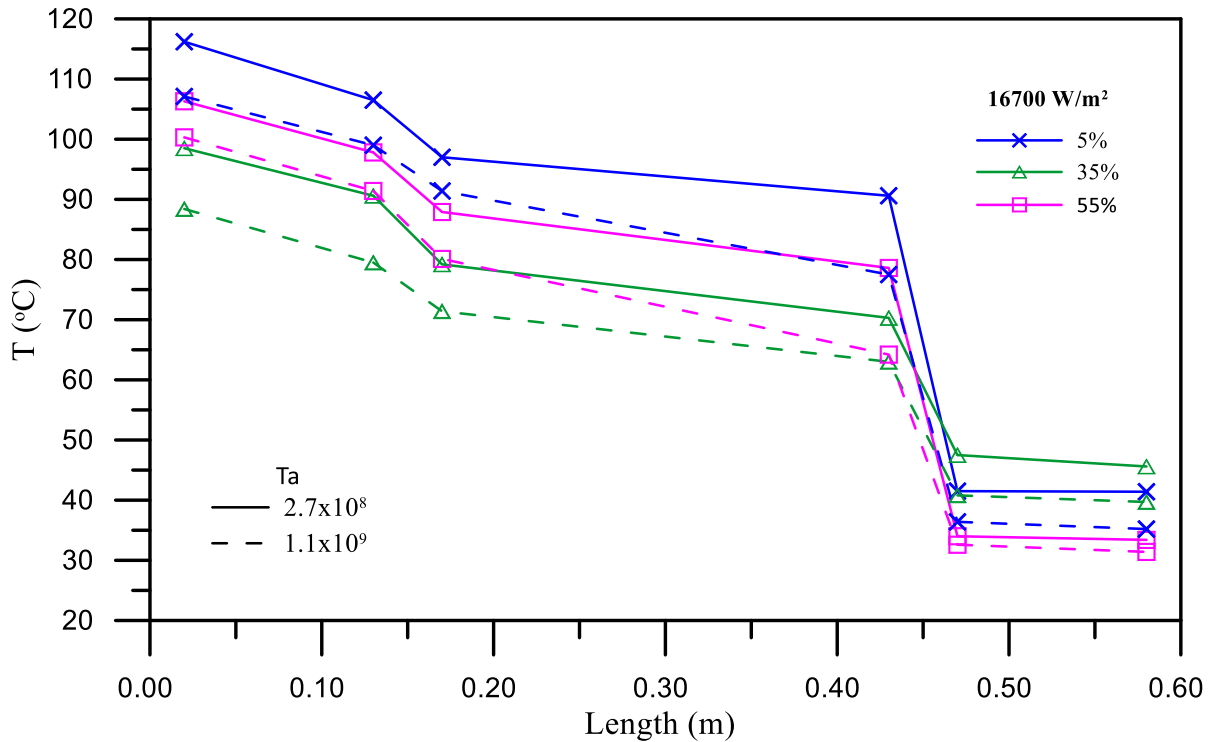
(b)

Fig. 8: Temperature distribution along the heat pipe for different charging ratios, Taylor numbers, and heat fluxes of (a) 10440 and (b) 16700 W/m².

Figure 9 presents the temperature difference between the evaporator and condenser against the charging ratio for the tested heat flux and Taylor numbers. Fig. 9 is split into two frames to avoid interference with the presented data and facilitate the visual observations of the results. Upon examination of Figs. 9a and 9b, it is evident that a 35% charge yields the lowest temperature difference between the condenser and evaporator, resulting in enhanced performance for rotating heat pipes.

In summary, low filling charges may increase the chance of the "dry out" phenomenon, which can raise the temperature of the evaporator and the temperature difference, leading to deteriorated performance, particularly for high heat flux (refer to Fig. 8b). Conversely, high filling charges can cause "flooding" hampering the condensation process and leading to deteriorated performance, particularly for low heat flux (refer to Fig. 8a). Therefore, based on the examined ranges of Taylor number and heat flux, the optimal charge level for heat pipe is approximately 35%. These results highlight the critical role of the charge ratio in the design and optimization of heat pipe systems.

Fig. 9: Temperature difference between evaporator and condenser at different charging ratios, Taylor Numbers, and heat fluxes of (a) 10440 and (b) 16700 W/m².

The effect of the filling ratio on the thermal performance of the axially rotating heat pipe is depicted in Fig. 10a, for thermal resistance and Fig. 10b, for the effective thermal conductivity. As observed in Fig. 10a, the filling ratio of 35% is the optimum liquid filling ratio that minimizes thermal resistance. For liquid filling ratios higher or lower than this value, the thermal resistance of the heat pipe increases. The trend partially agrees with the findings of He et al. [49]. Also, the effective thermal conductivity is optimum at a filling ratio of 35%, as presented in Fig. 10b. Therefore, both thermal resistance and effective thermal conductivity confirm that the optimum performance is attained at a filling ratio of 35% of the inner volume of the heat pipe, which is equivalent to about 140% of the evaporator volume. The finding is in partial agreement with the results of Panchal [38], who reported an increase in the heat pipe performance as the filling charge increased from 83 to 100% of the evaporator volume.
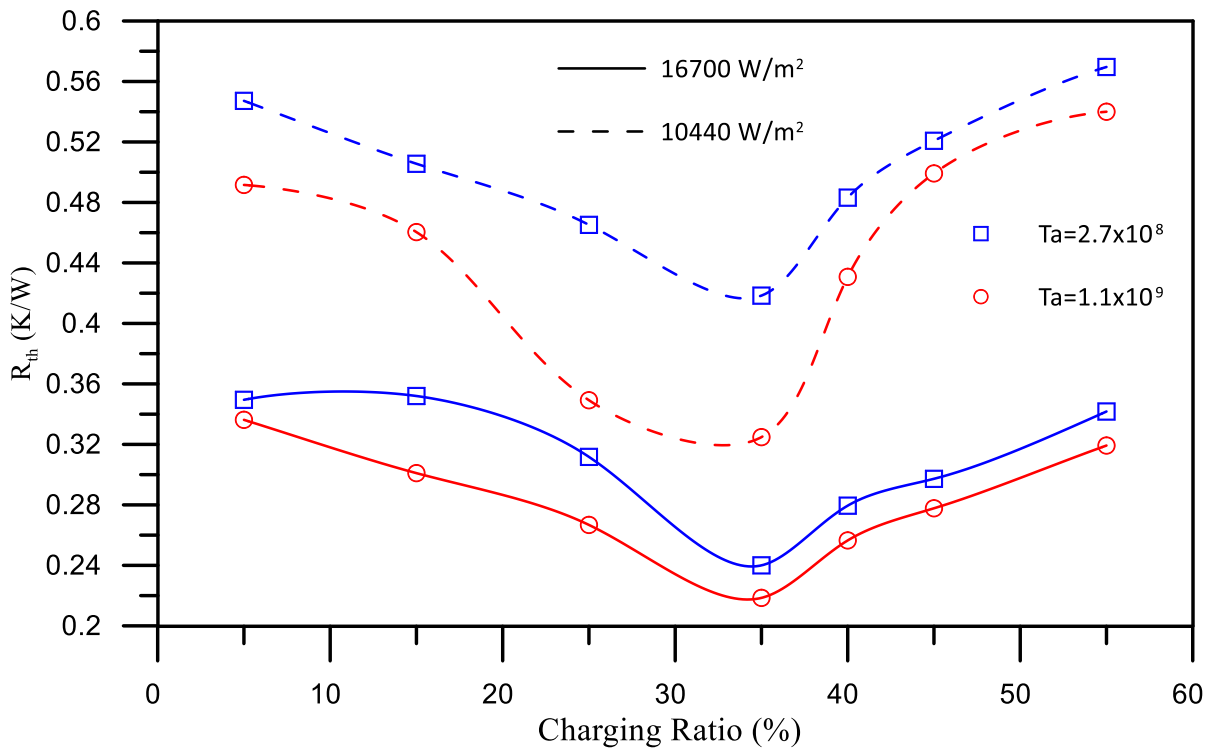
(a)
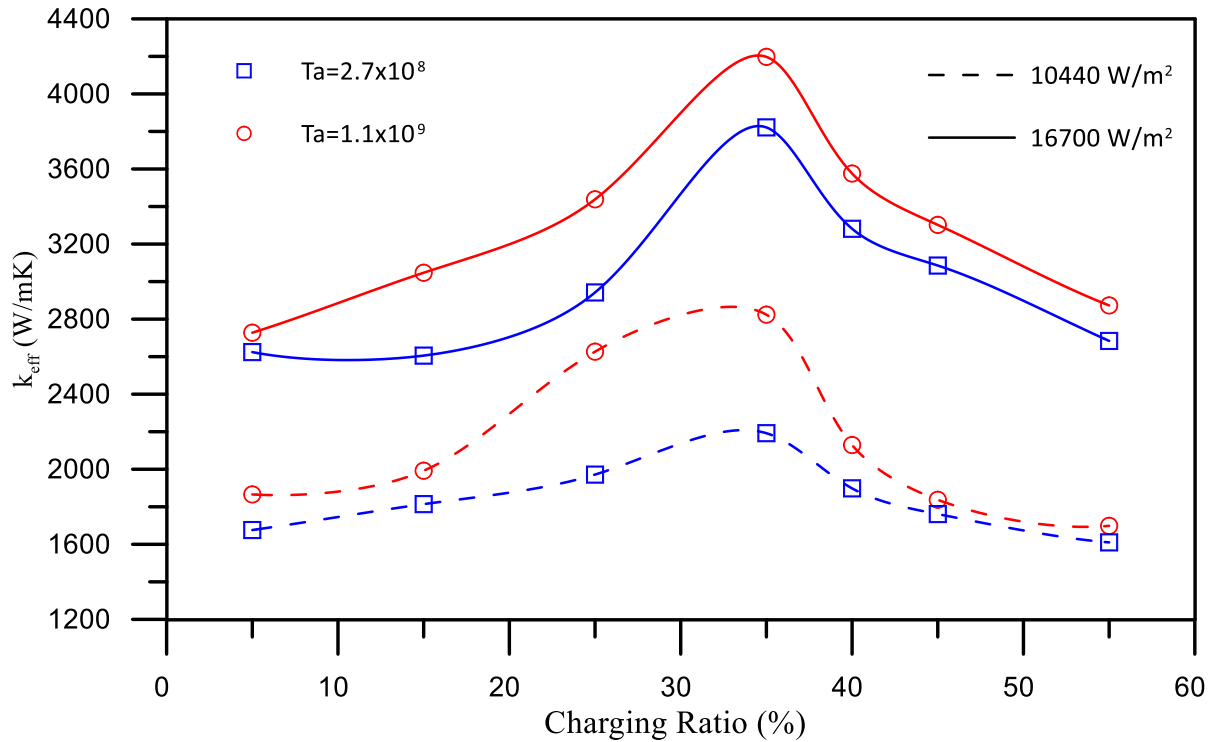
(b)

Fig. 10: The thermal resistance and effective thermal conductivity of the heat pipe at different Taylor numbers, heat fluxes, and charging ratios.

4. CONCLUSION

The present work reports the experimental performance of axially rotating horizontal heat pipes. A heat pipe was designed, constructed, and tested to conduct the investigation. The effects of rotational speed (ranging from 250 to 1500 rpm), heat flux (between 2090 and 16700 W/m^2), Taylor number (from 3.0×10^7 to 1.1×10^9), and the liquid filling ratio between 5 and 55% of the total interior volume of the heat pipe were examined and discussed. Based on the reported results, the following conclusions may be drawn.

- Higher Taylor numbers (or rotational speeds) lead to better performance of heat pipes in terms of low thermal resistances and high thermal conductivities compared to lower Taylor numbers. As the Taylor number increases from 3.0×10^7 to 1.1×10^9, the thermal resistance decreases by approximately 44.75% for low heat flux and 24.25% for high heat flux. The effective thermal conductivity of heat pipes increases by 30-40% for heat

fluxes ranging from 2090 to 8350 W/m^2 and about 20% for higher heat fluxes.

- The heat pipe demonstrates better thermal performance at low heat inputs compared to medium inputs. The lowest heat pipe performance occurs at heat fluxes ranging from approximately 7000 to 10000 W/m^2, depending on the Taylor number.

- The tested heat pipe outperforms a copper rod of the same dimensions by a factor of 4.3 to 9.47, depending on the heat flux (4.3-fold improvement for medium heat flux and 9.47-fold improvement for low heat flux).

- The liquid charge plays a critical role in the design and optimization of heat pipes. Within the examined ranges of Taylor number and heat flux, the optimum liquid charge for the heat pipe is approximately 35% of the inner pipe volume or 140% of the evaporator volume.

- The temperature difference between the evaporator and condenser decreases by approximately 43% (for the lowest heat flux of 2090 W/m^2) and 23% (for the highest heat flux of 16700 W/m^2) as the rotational speed increases from 250 to 1500 rpm. This highlights the significant impact of heat pipe rotation on reducing the temperature difference between the evaporator and condenser, especially at low heat flux.

Nomenclature

A_{cross}	Cross section area (m^2)
c	Condenser
c_p	Specific heat at constant pressure (J /kg K)
g	Gravitational acceleration (m/s^2)
h_{fg}	Heat of vaporization (J/kg)
k	Thermal conductivity (W/mK)
L	Heat pipe length (m)
N	Rotational speed (rpm)
q	Heat flux (W/m^2)
Q	Heat transfer rate (W)
R_{th}	Thermal resistance (K/W)
T	Temperature (K)

Greek letter

ρ	Density (kg/m^3)
σ	Surface tension coefficient (N/m)
μ	Dynamic viscosity (kg/ m s)

Subscript

c	Condenser section
e	Evaporator section
eff	Effective
l	Liquid
v	Vapor

REFERENCES

1. F. Song, D. Ewing, and C. Ching, Experimental investigation on the heat transfer characteristics of axial rotating heat pipes. International Journal of Heat and Mass Transfer, 2004. 47(22): p. 4721-4731.

2. R. Bertossi, N. Guilhem, V. Ayel, C. Romestant, and Y. Bertin, Modeling of heat and mass transfer in the liquid film of rotating heat pipes. International journal of thermal sciences, 2012. 52: p. 40-49.

3. Q. Su, S. Chang, M. Song, Y. Zhao, and C. Dang, An experimental study on the heat transfer performance of a loop heat pipe system with ethanol-water mixture as working fluid for aircraft anti-icing. International Journal of Heat and Mass Transfer, 2019. 139: p. 280-292.

4. S. Shittu, G. Li, X. Zhao, J. Zhou, X. Ma, and Y.G. Akhlaghi, Experimental study and exergy analysis of photovoltaic-thermoelectric with flat plate micro-channel heat pipe. Energy Conversion and Management, 2020. 207: p. 112515.

5. C. Wang, L. Zhang, X. Liu, S. Tang, S. Qiu, and G. Su, Experimental study on startup performance of high temperature potassium heat pipe at different inclination angles and input powers for nuclear reactor application. Annals of nuclear energy, 2020. 136: p. 107051.

6. Z. Li, M. Sarafraz, A. Mazinani, H. Moria, I. Tlili, T.A. Alkanhal, M. Goodarzi, and M.R. Safaei, Operation analysis, response and performance evaluation of a pulsating heat pipe for low temperature heat recovery. Energy Conversion and Management, 2020. 222: p. 113230.

7. J. Li, G. Zhou, T. Tian, and X. Li, A new cooling strategy for edge computing servers using compact looped heat pipe. Applied Thermal Engineering, 2021. 187: p. 116599.

8. J. Lee and S.J. Kim, Effect of channel geometry on the operating limit of micro pulsating heat pipes. International Journal of Heat and Mass Transfer, 2017. 107: p. 204-212.

9. C. Guo, T. Wang, C. Guo, Y. Jiang, S. Tan, and Z. Li, Effects of filling ratio, geometry parameters and coolant temperature on the heat transfer performance of a wraparound heat pipe. Applied Thermal Engineering, 2022. 200: p. 117724.

10. K. Desai, G. Lakra, R. Rajesh, and S.S. Prabu, Investigation on the effect of thermal properties by changing geometry of a heat pipe using simulation. Materials Today: Proceedings, 2021. 46: p. 8473-8479.

11. H.A. Machado and R.F. de Miranda, Operation limits for rotating cylindrical heat pipes. Numerical Heat Transfer: Part A: Applications, 2003. 44(3): p. 299-313.

12. P. Nemec, A. Čaja, and M. Malcho, Mathematical model for heat transfer limitations of heat pipe. Mathematical and Computer Modelling, 2013. 57(1-2): p. 126-136.

13. C. Busse, Theory of the ultimate heat transfer limit of cylindrical heat pipes. International Journal of Heat and Mass Transfer, 1973. 16(1): p. 169-186.

14. M. Mansour, Mathematical model for heat transfer limitations of heat pipe. IJEAT, 2016. 5(4).

15. A. Faghri, Heat pipe science and technology. 1995: Global Digital Press.
16. A. Jiao, R. Riegler, H. Ma, and G. Peterson, Thin film evaporation effect on heat transport capability in a grooved heat pipe. Microfluidics and Nanofluidics, 2005. 1: p. 227-233.
17. R.R. Riehl and N. dos Santos, Loop heat pipe performance enhancement using primary wick with circumferential grooves. Applied Thermal Engineering, 2008. 28(14-15): p. 1745-1755.
18. A.A. Yakomaskin, V.N. Afanasiev, N.N. Zubkov, and D.N. Morskoy, Investigation of heat transfer in evaporator of microchannel loop heat pipe. Journal of heat transfer, 2013. 135(10).
19. R. Hodot, V. Sartre, F. Lefevre, and C. Sarno, 3D modeling and optimization of a loop heat pipe evaporator. Heat Pipe Science and Technology, An International Journal, 2014. 5(1-4).
20. W.-W. Wang, Y. Cai, L. Wang, C.-W. Liu, F.-Y. Zhao, and D. Liu, Thermo-hydrodynamic analytical model, numerical solution and experimental validation of a radial heat pipe with internally finned condenser applied for building heat recovery units. Energy Conversion and Management, 2020. 219: p. 113041.
21. J. Kim and S.J. Kim, Experimental investigation on the effect of the condenser length on the thermal performance of a micro pulsating heat pipe. Applied Thermal Engineering, 2018. 130: p. 439-448.
22. J. Kim and S.J. Kim, Experimental investigation on working fluid selection in a micro pulsating heat pipe. Energy Conversion and Management, 2020. 205: p. 112462.
23. R. Singh, A. Akbarzadeh, and M. Mochizuki, Effect of wick characteristics on the thermal performance of the miniature loop heat pipe. Journal of heat transfer, 2009. 131(8).
24. T. Shioga, Y. Mizuno, and H. Nagano, Operating characteristics of a new ultra-thin loop heat pipe. International Journal of Heat and Mass Transfer, 2020. 151: p. 119436.
25. Y. Ji, H. Ma, F. Su, and G. Wang, Particle size effect on heat transfer performance in an oscillating heat pipe. Experimental Thermal and Fluid Science, 2011. 35(4): p. 724-727.
26. H. Ma, C. Wilson, B. Borgmeyer, K. Park, Q. Yu, S. Choi, and M. Tirumala, Effect of nanofluid on the heat transport capability in an oscillating heat pipe. Applied Physics Letters, 2006. 88(14): p. 143116.
27. Y. Cao, Miniature high-temperature rotating heat pipes and their applications in gas turbine cooling. Frontiers in Heat Pipes (FHP), 2010. 1(2).
28. M. Groll, H. Krahling, and W. Munzel, Heat pipes for cooling of an electric motor. Journal of Energy, 1978. 2(6): p. 363-367.
29. N. Putra and B. Ariantara, Electric motor thermal management system using L-shaped flat heat pipes. Applied Thermal Engineering, 2017. 126: p. 1156-1163.
30. S.-F. Li and Z.-h. Liu, Parametric study of rotating heat pipe performance: A review. Renewable and Sustainable Energy Reviews, 2020. 117: p. 109482.

31.   I. Voigt and W.-G. Drossel, Experimental investigation of heat pipe performance under translational acceleration. Heat and Mass Transfer, 2022. 58(2): p. 209-219.

32.   P.D. Dunn and D. Reay, Heat pipes. 2012: Elsevier.

33.   A.A. El-Nasr and S. El-Haggar, Effective thermal conductivity of heat pipes. Heat and Mass transfer, 1996. 32(1-2): p. 97-101.

34.   M. Xie, Z. Xue, W. Qu, and W. Li, Experimental investigation of heat transfer performance of rotating heat pipe. Procedia Engineering, 2015. 99: p. 746-751.

35.   W. Lian, W. Chang, and Y. Xuan, Numerical investigation on flow and thermal features of a rotating heat pipe. Applied Thermal Engineering, 2016. 101: p. 92-100.

36.   W. Chang, Y. Li, K. Fang, and F. Zhang. Numerical Simulation of two-phase Flow and Heat Transfer in an Axial Rotating Heat Pipe. in 2020 IEEE 5th Information Technology and Mechatronics Engineering Conference (ITOEC). 2020. IEEE.

37.   B. Denkena, B. Bergmann, K. Kono, R. Ishiguro, and H. Klemme, Characterization of heat conductivity of eccentrically rotating heat pipes used for cooling of motor spindles. 2021.

38.   R. N.Panchal, J. R.Panchal, and A.D. Awasare, Study of working fluid for heat pipe. International Journal of Computer Engineering and Applications, 2018. XII.

39.   J. Nonneman, B. Van der Sijpe, I. T'Jollyn, S. Vanhee, J. Druant, and M. De Paepe. Evaluation of High Performance Rotor Cooling Techniques for Permanent Magnet Electric Motors. in 2021 IEEE International Electric Machines & Drives Conference (IEMDC). 2021. IEEE.

40.   Z. Chen, Z. Yu, J. Fu, and B. Liu. Study of heat pipe in motor cooling: A review. in E3S Web of Conferences. 2021. EDP Sciences.

41.   Arai, T., M. Kawaji, and Y. Koito. Visualization of Two-Phase Flow in 3D Printed Polycarbonate Pulsating Heat Pipe With Aluminum Substrate. in International Conference on Nanochannels, Microchannels, and Minichannels. 2018. American Society of Mechanical Engineers.

42.   Eidan, A.A., M.J. Alshukri, M. Al-fahham, A. AlSahlani, and D.M. Abdulridha, Optimizing the performance of the air conditioning system using an innovative heat pipe heat exchanger. Case Studies in Thermal Engineering, 2021. 26: p. 101075.

43.   White, F.M., Fluid Mechanics, McGraw-Hill Series in Mechanical Engineering. 2011, McGraw Hill New York.

44.   Taylor, G., I·, Stability of a viscous liquid contained between two rotating cylinders, Phil. Transi. Roy. Soc. Lond. A, 1923. 223: p. 289-343.

45.   Fadhl, B., L.C. Wrobel, and H. Jouhara, Numerical modelling of the temperature distribution in a two-phase closed thermosyphon. Applied Thermal Engineering, 2013. 60(1-2): p. 122-131.

46.   Aboutalebi, M., A.N. Moghaddam, N. Mohammadi, and M. Shafii, Experimental investigation on performance of a rotating closed loop pulsating heat pipe. International communications in heat and mass transfer, 2013. 45: p. 137-145.

47. S Kline, F McClintock, Describing uncertainties in single-sample experiments. Mech. Eng., 1963. 75: p. 3-8.
48. R Moffat., Describing the uncertainties in experimental results. Experimental thermal and fluid science, 1988. 1(1): p. 3-17.
49. He, C., R. Zhao, and J. Zheng, Heat transfer performance of heat pipe rotating about parallel axes. Journal of Chong qing University, 2008. 31: p. 632-636.